

Internal Note No. 68-FM-4

U. H. ...



NATIONAL AERONAUTICS AND SPACE ADMINISTRATION
MSC INTERNAL NOTE NO. 68-FM-4

January 8, 1968

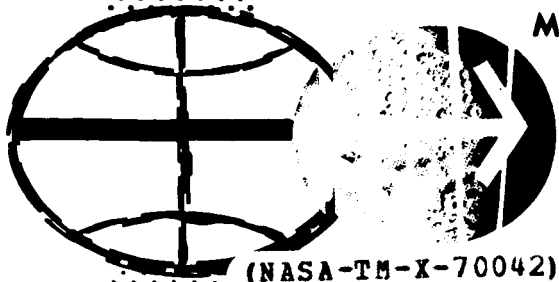
mi

TRAJECTORY INFORMATION FOR
INITIAL PLANNING OF TERMINAL
PHASE OF COELLIPTIC SEQUENCE
RENDEZVOUS IN LUNAR ORBIT

By James D. Alexander
and Mary T. Alexander,
Orbital Mission Analysis Branch

JUL 22 1969

Technical Library, Ballistics, Inc.



MISSION PLANNING AND ANALYSIS DIVISION
MANNED SPACECRAFT CENTER
HOUSTON, TEXAS

(NASA-TM-X-70042) TRAJECTORY INFORMATION
FOR INITIAL PLANNING OF TERMINAL PHASE
OF COELLIPTIC SEQUENCE RENDEZVOUS IN
LUNAR ORBIT (NASA) 22 p

N74-72483

00/99 Unclas
16839

MSC INTERNAL NOTE NO. 68-FM-4

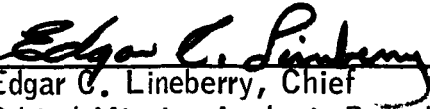
PROJECT APOLLO

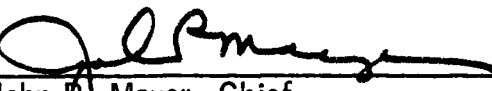
TRAJECTORY INFORMATION FOR INITIAL PLANNING OF
TERMINAL PHASE OF COELLIPTIC SEQUENCE
RENDEZVOUS IN LUNAR ORBIT

By James D. Alexander and Mary T. Alexander
Orbital Mission Analysis Branch

January 8, 1968

MISSION PLANNING AND ANALYSIS DIVISION
NATIONAL AERONAUTICS AND SPACE ADMINISTRATION
MANNED SPACECRAFT CENTER
HOUSTON, TEXAS

Approved: 
Edgar C. Lineberry, Chief
Orbital Mission Analysis Branch

Approved: 
John P. Mayer, Chief
Mission Planning and Analysis Division

FIGURES

Figure		Page
1	Elevation angle (chaser-to-target vehicle) at TPI for "line-of-sight TPI" as a function of coelliptic Δh	8
2	Terminal phase ΔV -vector magnitudes as a function of coelliptic Δh	9
3	Terminal phase ΔV -component magnitudes as a function of coelliptic Δh	10
4	Phase angle (target-vehicle-ahead) at TPI as a function of coelliptic Δh	11
5	Vehicle-to-vehicle range at TPI as a function of coelliptic Δh	12
6	Orbital apsides changes resulting from TPI as a function of coelliptic Δh	13
7	Terminal phase true anomalies as a function of coelliptic Δh	14
8	Terminal phase flight-path angles as a function of coelliptic Δh	15
9	Terminal phase relative motion curves (target-vehicle-centered curvilinear coordinate system). . .	16
10	Terminal phase time histories of elevation angle (chaser-to-target vehicle)	17
11	Terminal phase time histories of phase angle (target-vehicle-ahead)	18
12	Terminal phase time histories of vehicle-to-vehicle range.	19

TRAJECTORY INFORMATION FOR INITIAL PLANNING OF
TERMINAL PHASE OF COELLIPTIC SEQUENCE

RENDEZVOUS IN LUNAR ORBIT

By James D. Alexander and Mary T. Alexander

SUMMARY AND INTRODUCTION

This note presents figures which contain information pertaining to the terminal phase of the coelliptic sequence rendezvous in lunar orbit. Although the data were generated by a Keplerian method, the information is sufficiently accurate for initial planning of lunar orbit rendezvous.

The terminal phase of a coelliptic sequence rendezvous begins with the maneuver which places the chaser vehicle on an intercept trajectory with the target vehicle; this maneuver is referred to as terminal phase initiation (TPI). Theoretically, the rendezvous terminal phase is completed by an impulsive velocity match maneuver at the intercept of the two vehicles; this maneuver is referred to as terminal phase finalization (TPF). Operationally, however, the intercept velocity match is effected by a series of braking maneuvers which are based on range/range-rate schedules and are controlled manually. The operational propellant requirement for these braking maneuvers is usually about 1.5 to 2.0 times the theoretical velocity-match requirement.

The time duration of the (theoretical) terminal phase is a function of the selected central angle of travel of the target vehicle during terminal phase. This central angle is currently a standard 140° . The targeting of TPI incorporates the corresponding theoretical TPI-to-TPF Δt , which ranges from about 44 to 48 minutes depending on the length of the target vehicle's semimajor axis. Also, nominally-zero midcourse correction maneuvers (based on effecting intercept at the original TPF time) will be scheduled at fixed Δt 's from TPI, usually at about 15 and 30 minutes after TPI.

The data presented herein are for a theoretical terminal phase - i.e., a perfectly-executed (impulsive) TPI followed by a perfectly-executed (impulsive) TPF, with no perturbations or dispersions involved.

DEFINITIONS

Symbols and Abbreviations

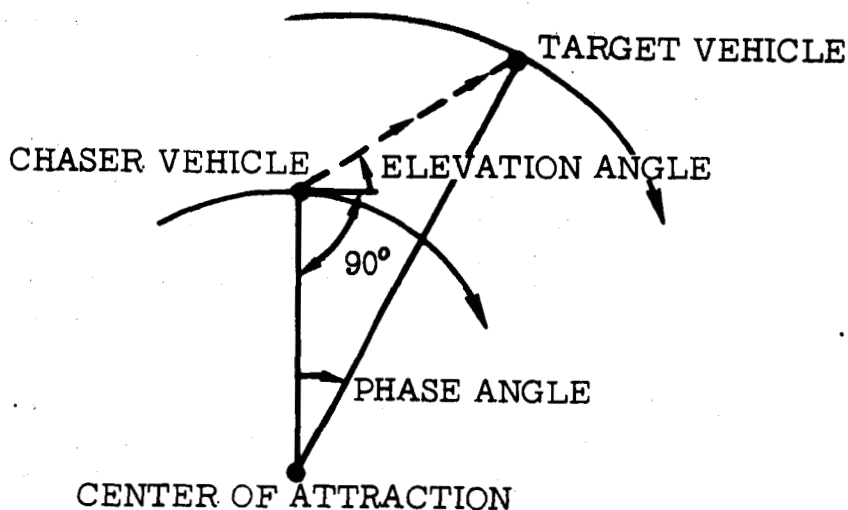
Δh	difference in the lengths of the two vehicles' radii.
ΔV	velocity increment.
φ_T	target vehicle's central angle of travel during terminal phase.
TPI	"terminal phase initiation"; establishment of intercept trajectory.
TPF	"terminal phase finalization"; theoretical velocity match at intercept - impulsive equivalent of braking.

Terms

Coelliptic Δh	Constant Δh during phase preceding TPI.
Curvilinear coordinates ^a	The vertical coordinate is the difference in the lengths of the two vehicles' radii (i.e., Δh); the horizontal coordinate is the arc length between the two vehicles' radii, measured at the radius length of the vehicle in which the coordinate system is centered.
Elevation angle ^a	Angle (measured counterclockwise) between a vehicle's local horizontal in the direction of motion and the line-of-sight to the other vehicle.

^aFor non-coplanar situations, the parameter is measured by projecting the position of one vehicle into the other vehicle's plane.

Flight-path angle	Angle between a vehicle's local horizontal in the direction of motion and its velocity vector (positive when the velocity vector is above the local horizontal).
"Line-of-sight TPI"	TPI for which the direction of the impulsive ΔV vector is along the instantaneous line-of-sight to the target vehicle.
Phase angle ^a	Central angle between the two vehicles' radii.



DESCRIPTION OF FIGURES

The data presented in the figures are based on the following constants and assumptions:

- A "line-of-sight TPI". (See definitions.)
- Impulsive, undispersed burns.
- The target vehicle's central angle of travel during terminal phase (φ_T) is 140° .
- The target vehicle is in an 80-n. mi. circular orbit for all data with the chaser below; for chaser above, the target vehicle's circular orbit altitude varies from 80 to 30 n. mi. as the coelliptic Δh varies from near 0 to 50 n. mi.

^aFor non-coplanar situations, the parameter is measured by projecting the position of one vehicle into the other vehicle's plane.

- e. The chaser vehicle is in a circular orbit prior to TPI.
- f. Coelliptic Δh 's are from near 0 to 50 n. mi. for both chaser below and chaser above.
- g. Coplanar vehicular planes.
- h. A moon mean radius of 5 702 395 ft; a moon gravitational constant of $1.7314 \times 10^{14} \text{ ft}^3/\text{sec}^2$.

Figure 1 presents the chaser-to-target-vehicle elevation angle required at TPI for a "line-of-sight TPI" as a function of coelliptic Δh . It is seen that the "line-of-sight TPI" elevation angle varies by only about 2° as the coelliptic Δh varies from 15 to 50 n. mi. for both chaser below and chaser above. Actually, the elevation angle for a specific coelliptic Δh with the chaser above is approximately equal to the corresponding chaser-below value plus 180° plus the absolute value of phase angle.

The magnitudes of the ΔV vector at TPI and at TPF (along with the sum of these two magnitudes) are shown in figure 2 as a function of coelliptic Δh . It is noted that the chaser-above values are continuously larger than the corresponding chaser-below values, although the differences are nearly negligible for the smaller coelliptic Δh 's.

Shown in figure 3 are the ΔV -component (horizontal and vertical at both TPI and TPF) magnitudes as a function of coelliptic Δh . The positive horizontal is in the direction of motion, and the positive vertical is away from the center of attraction. It is seen that as the coelliptic Δh increases the vertical component at TPF increases considerably more rapidly than the vertical component at TPI for both chaser below and chaser above. Also, although there is no significant difference between corresponding chaser-below and chaser-above horizontal components, there is a significant difference between corresponding chaser-below and chaser-above vertical components. This latter difference is due to the difference in the chaser's transfer angle for corresponding chaser-below and chaser-above Δh 's. Similar effects in the curves of several of the other figures are due to this difference in transfer angles.

Each as a function of coelliptic Δh , phase angle (target-vehicle-ahead) at TPI is shown in figure 4, and the vehicle-to-vehicle range at TPI is shown in figure 5. It is seen that for both of these variables there is essentially no difference between corresponding chaser-below and chaser-above values.

Changes in the orbital apsides resulting from TPI are shown as a function of coelliptic Δh in figure 6. It is seen that the resulting apsidal altitudes are only slightly different from the altitudes of the two vehicles' orbits prior to TPI for both chaser-below and chaser-above cases.

Figure 7 shows true anomaly instantaneously after TPI and instantaneously before TPI as a function of coelliptic Δh . Corresponding flight-path angle data are shown in figure 8.

Presented in figure 9 are terminal phase relative motion curves in a target-vehicle-centered curvilinear coordinate system for coelliptic Δh 's of 15, 30, and 50 n. mi. (chaser above and chaser below). Ten-minute time ticks are shown relative to TPI.

Figures 10, 11, and 12 show terminal phase time histories (with zero time at TPI and with curves for coelliptic Δh 's of 15, 30, and 50 n. mi., chaser below and chaser above) for the following parameters: chaser-to-target-vehicle elevation angle (figure 10), target-vehicle-ahead phase angle (figure 11), and vehicle-to-vehicle range (figure 12). The nearly negligible differences in corresponding chaser-below and chaser-above curves in figures 9 through 12 are due to the difference in transfer angles (explained above) and the difference in the target vehicle orbital altitudes. It is seen that the variation between the elevation angle curves is nearly negligible throughout terminal phase regardless of Δh for either chaser below or chaser above. This lack of variation is a basic component of the terminal phase of coelliptic sequence rendezvous.

As stated above, the data presented in each of the figures are based on exact "line-of-sight TPI's", for which the associated elevation angle is slightly a function of coelliptic Δh . The use of a standard (or average) TPI elevation angle for all chaser-below (or all chaser-above) coelliptic Δh 's instead of the exact "line-of-sight" value results in nearly negligible variations for the type of data presented here. Under real-time conditions therefore, in order to simplify procedures, a standard TPI elevation angle will probably be incorporated - for example, a TPI elevation angle of 26° for all chaser-below cases regardless of coelliptic Δh .

Other nearly negligible variations in the data will result due to finite thrusting instead of impulsive burns. Also, slight variations in the data would result due to a slightly elliptical target orbit or a noncoplanar situation.

The φ_T of 140° is the current standard for all of the coelliptic sequence rendezvous in the Apollo missions. This φ_T is large enough to allow sufficient time for two terminal phase midcourse corrections in lunar orbit and to normally not require excessive ΔV ; it is sufficiently less than 180° to avoid "singularity" out-of-plane problems.

The coelliptic Δh range is sufficiently large to cover all feasible lunar orbit rendezvous situations. The probable coelliptic Δh range for nominal and contingency situations is about 10 to 30 n. mi., with chaser below or above.

In generating the data for the chaser-above cases, the altitude of the target vehicle's circular orbit was decreased as the coelliptic Δh increased in an attempt to reflect the more probable chaser-above situations - namely, rescue situations. In other words, for a chaser-above coelliptic Δh between 40 and 50 n. mi., the target altitude would probably be between 20 and 40 n. mi. instead of between 60 and 80 n. mi.

Finally, it should be emphasized that no significant changes result in the type of data presented for variations in the target orbit altitude up to about 30 n. mi.

CONCLUDING REMARKS

Most recently a decrease in the altitude of the nominal CSM parking orbit for the lunar orbit phase of the first lunar landing mission from 80 to 60 n. mi. has become highly probable. As previously emphasized, however, the data presented for the 80 n. mi. target orbit altitude is essentially as accurate for a 60 n. mi. target orbit altitude as for an 80 n. mi. target orbit altitude. Also, if the pre-TPI conditions and the terminal phase parameters assumed herein are incorporated, the terminal phase values are a function only of the coelliptic Δh (mainly) and of the target orbit altitude (slightly) - i.e., the terminal phase values are otherwise independent of the sequence prior to TPI.

Although the information presented herein is theoretical and does not involve perturbations or dispersions, by supplementing it with various operational factors such as that for braking, it can be of considerable value for initial planning of lunar orbit rendezvous.

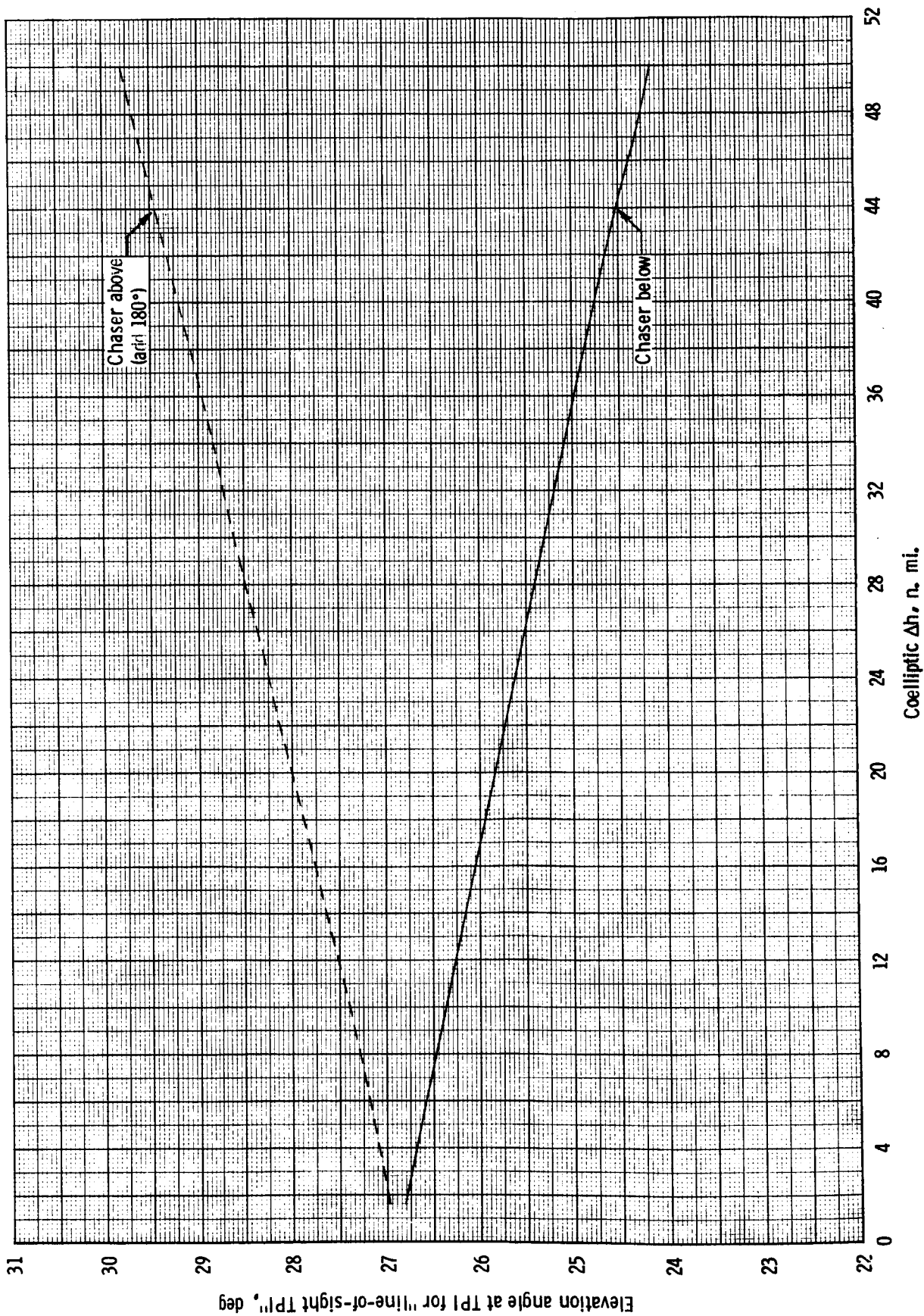


Figure 1. - Elevation angle (chaser-to-target vehicle) at TPI for "line-of-sight TPI" as a function of coelliptic Δh .

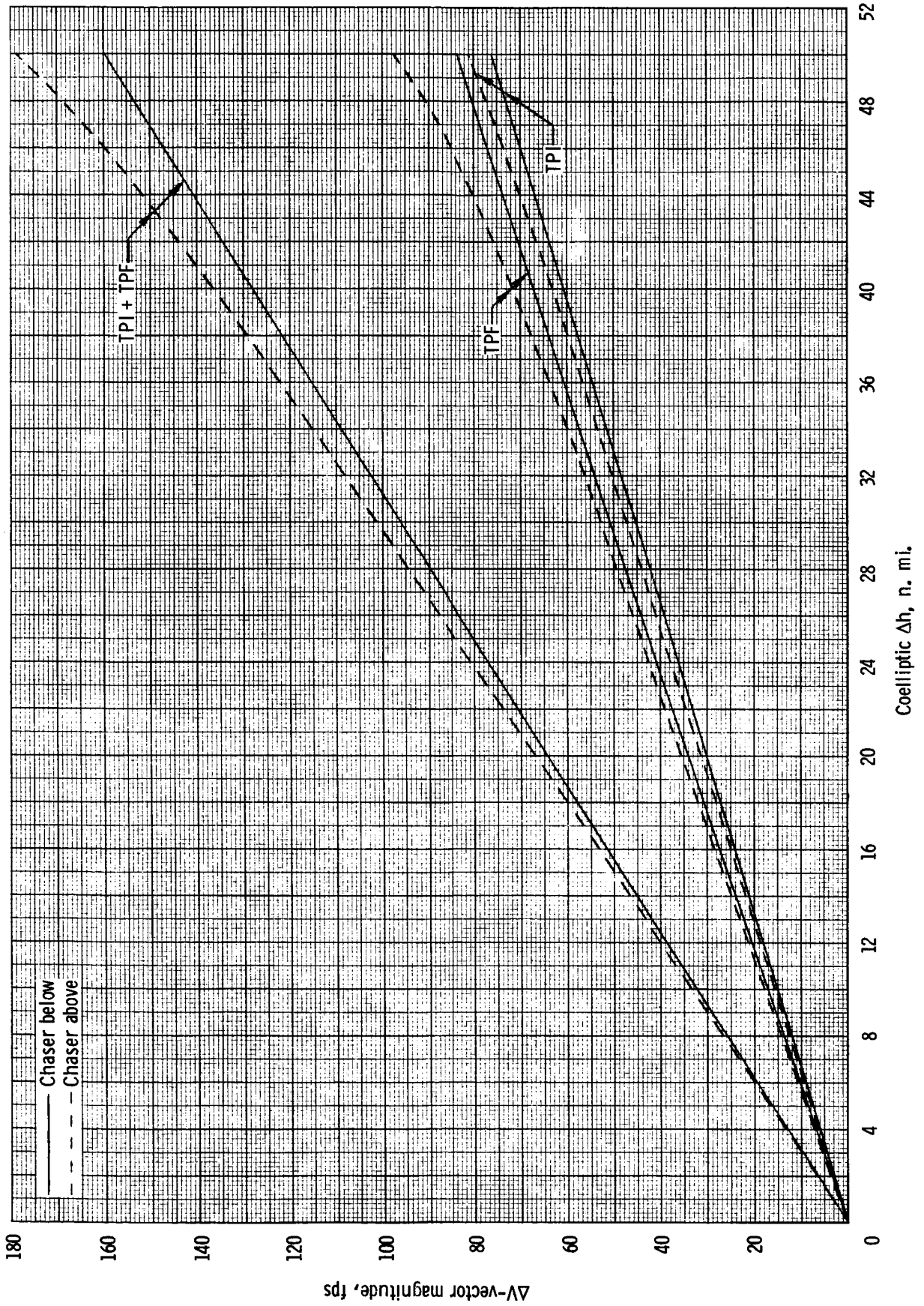


Figure 2. - Terminal phase ΔV -vector magnitudes as a function of coelliptic Δh .

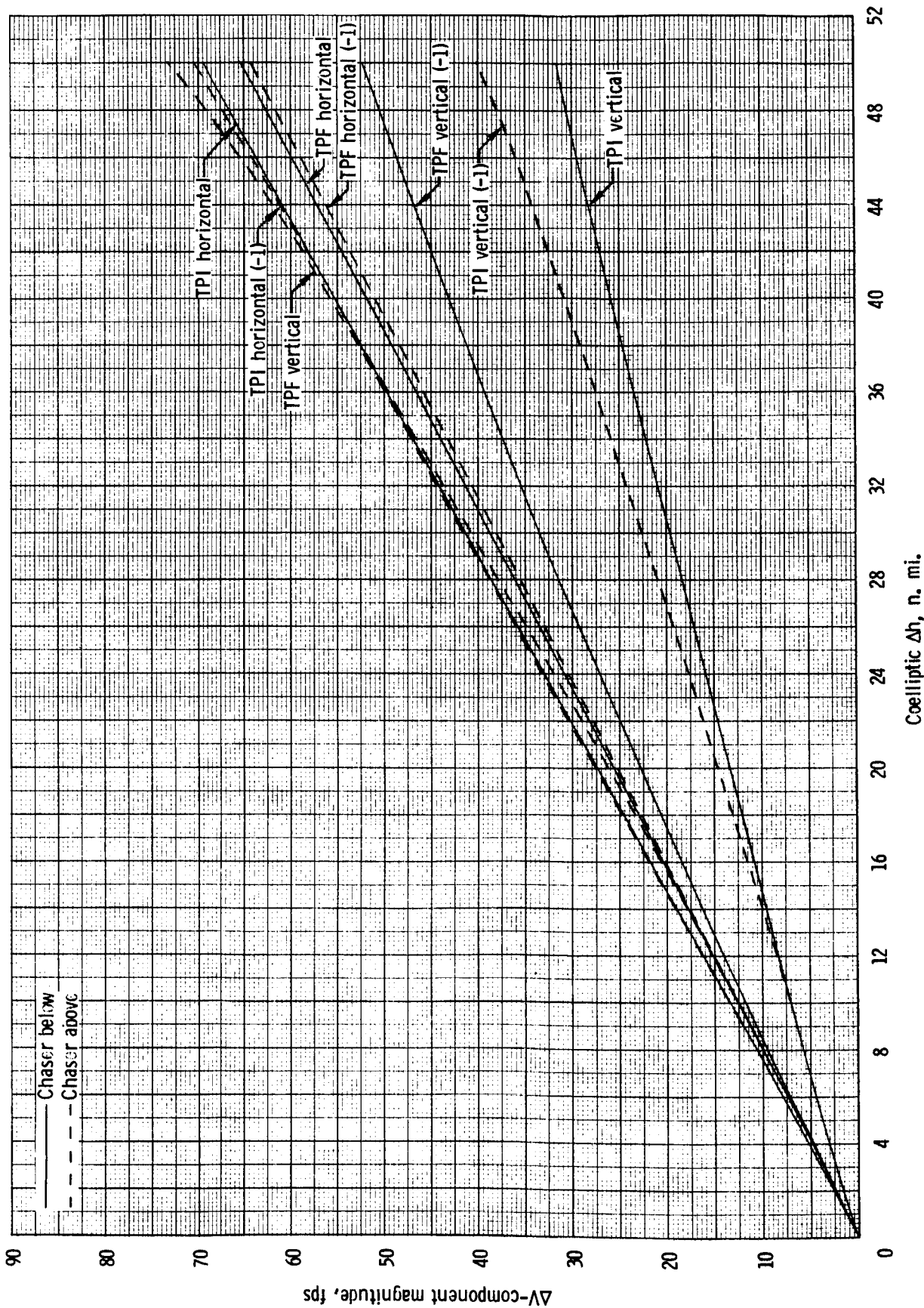


Figure 3. - Terminal phase ΔV -component magnitudes as a function of coelliptic Δh .

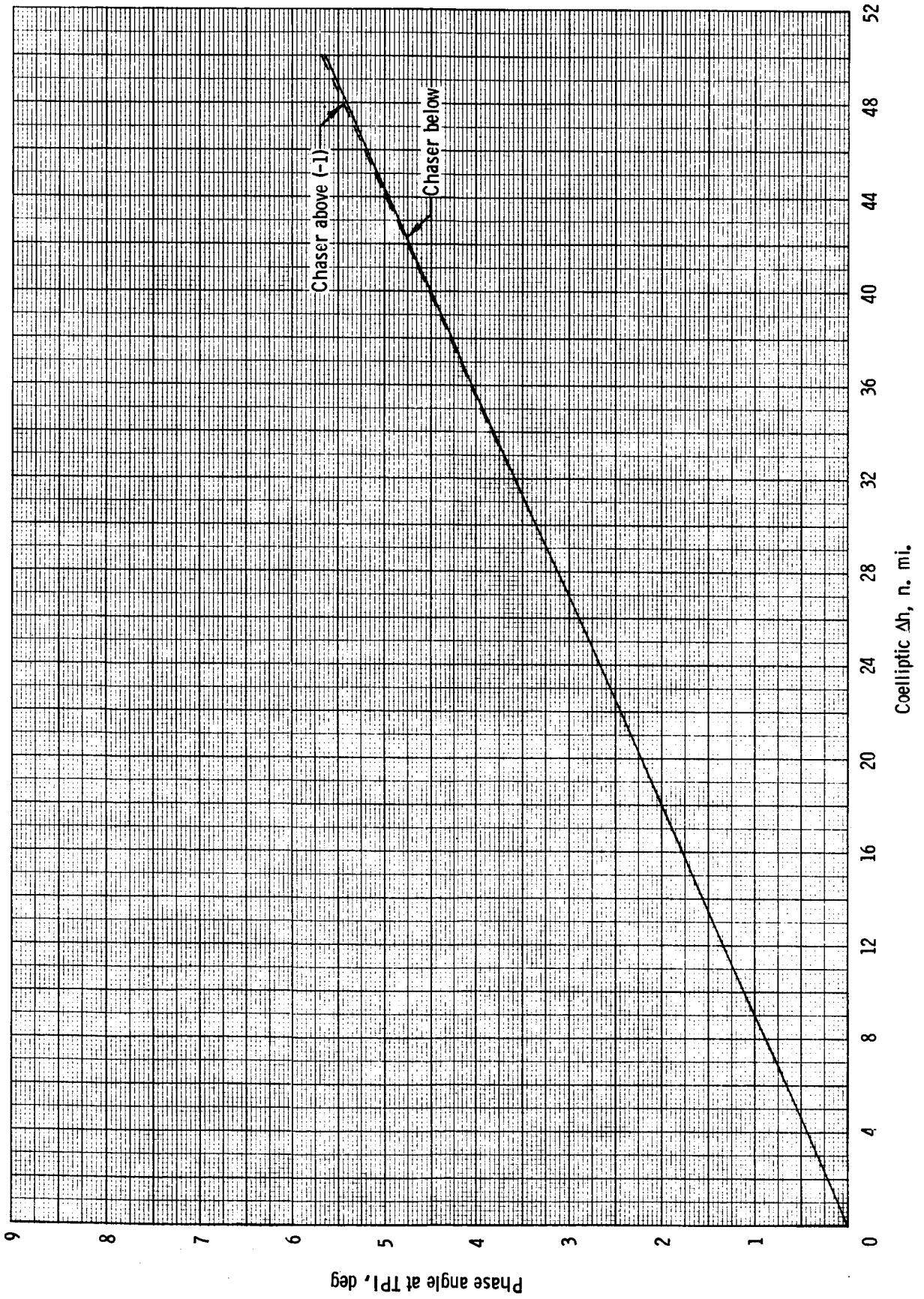


Figure 4. - Phase angle (target-vehicle-ahead) at TPI as a function of coelliptic Δh .

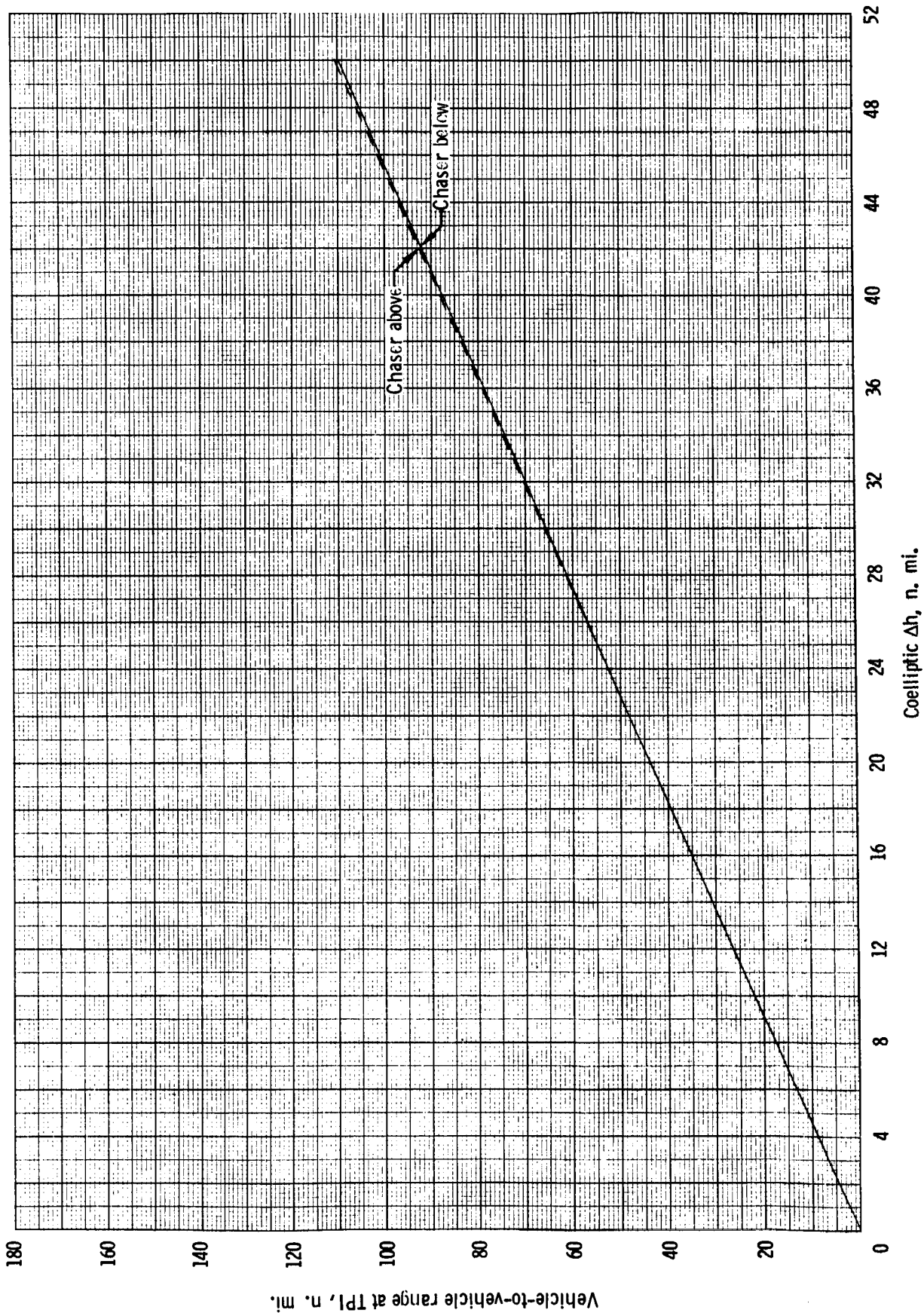
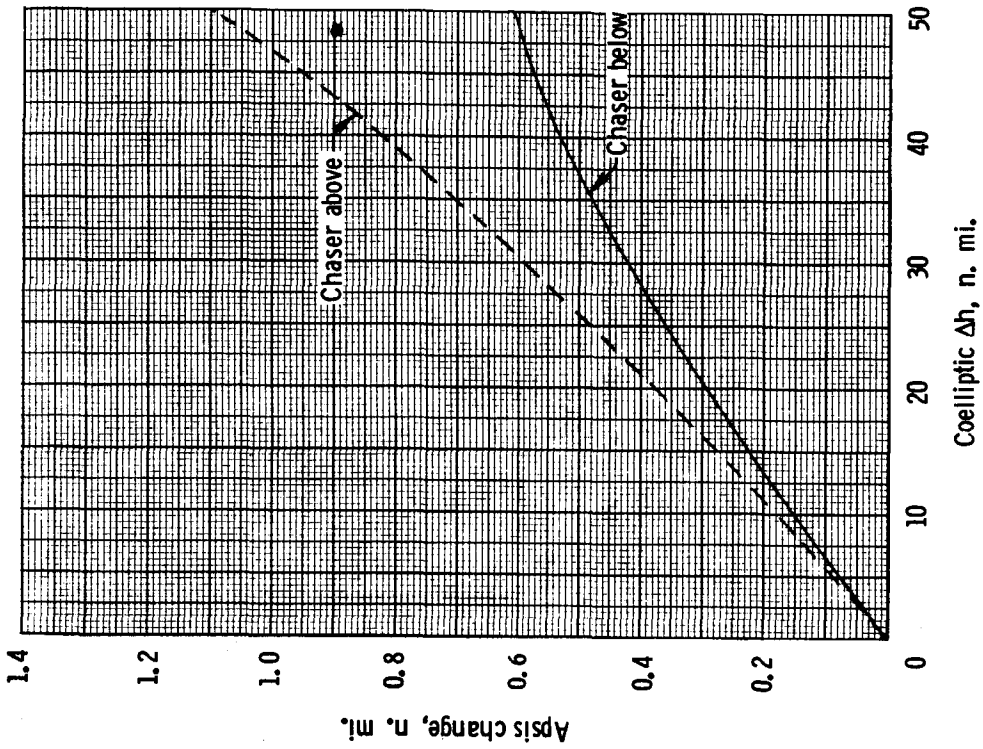
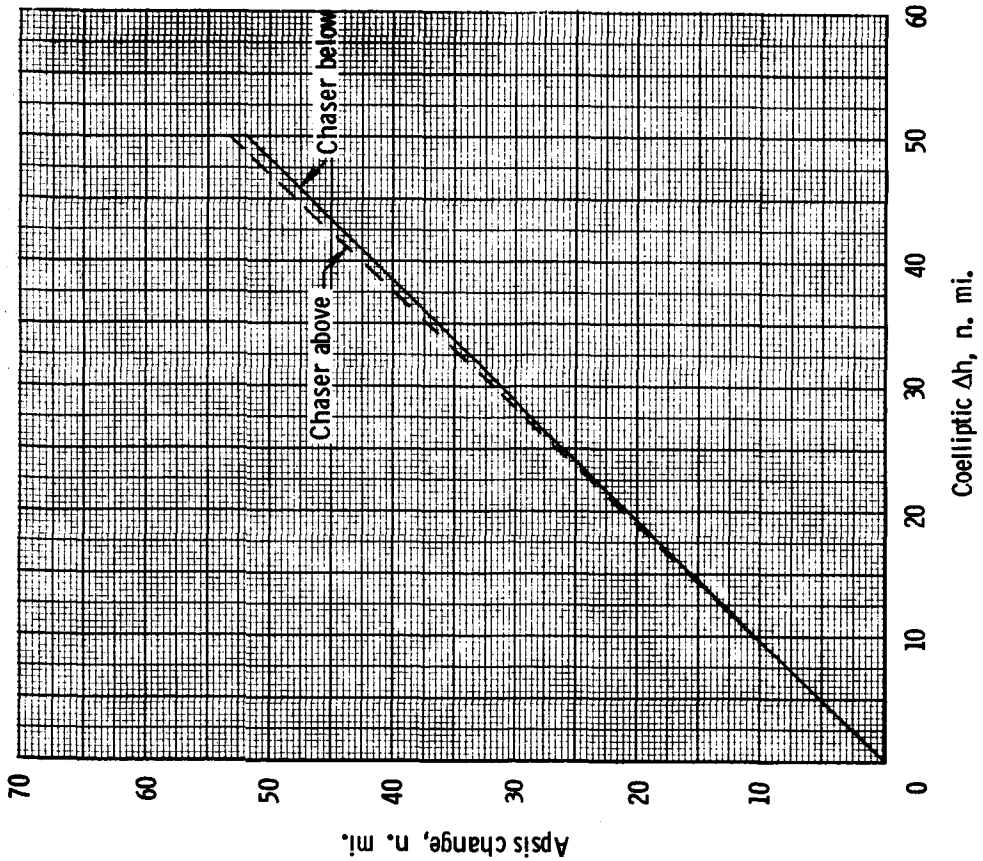


Figure 5. - Vehicle-to-vehicle range at TPI as a function of coelliptic Δh .

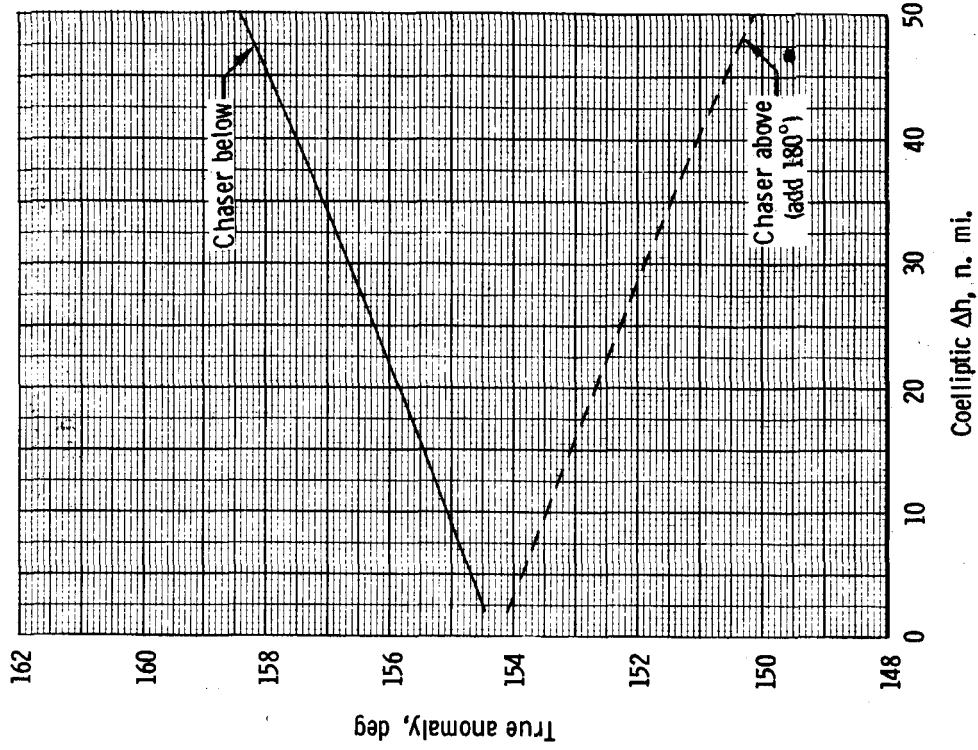


(a) Increase in apocynthion for chaser below;
decrease in pericynthion for chaser above.

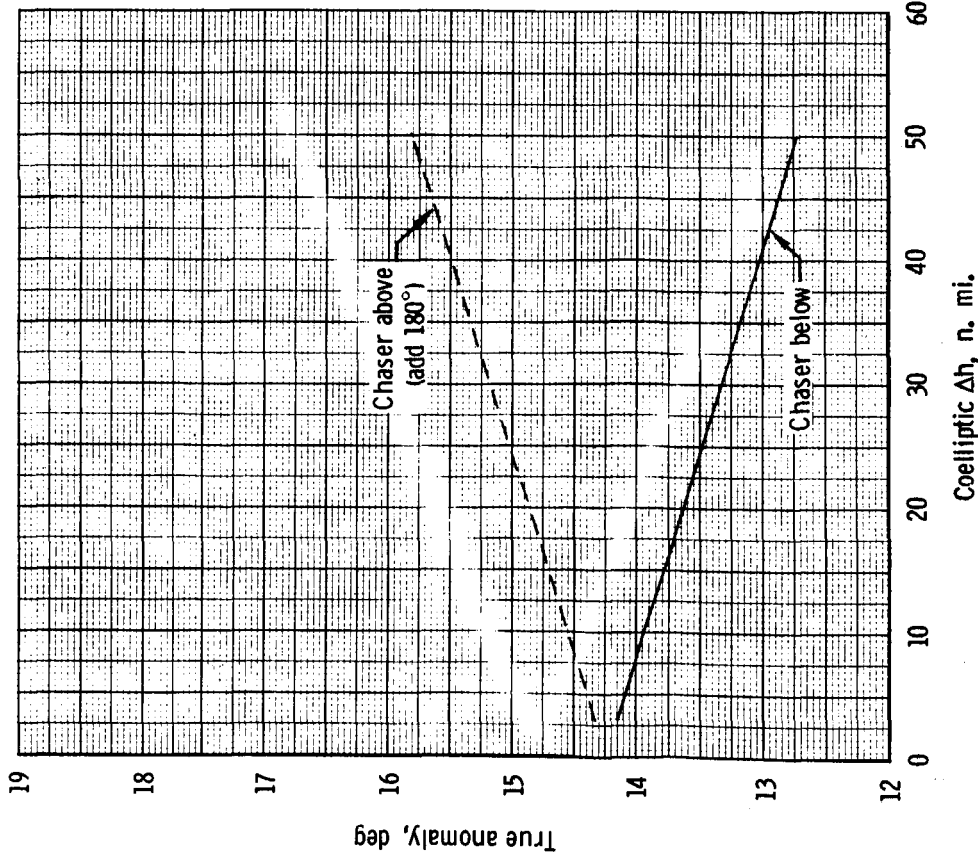


(b) Decrease in pericynthion for chaser below;
increase in apocynthion for chaser above.

Figure 6. - Orbital apsides changes resulting from TPI as a function of coelliptic Δh .

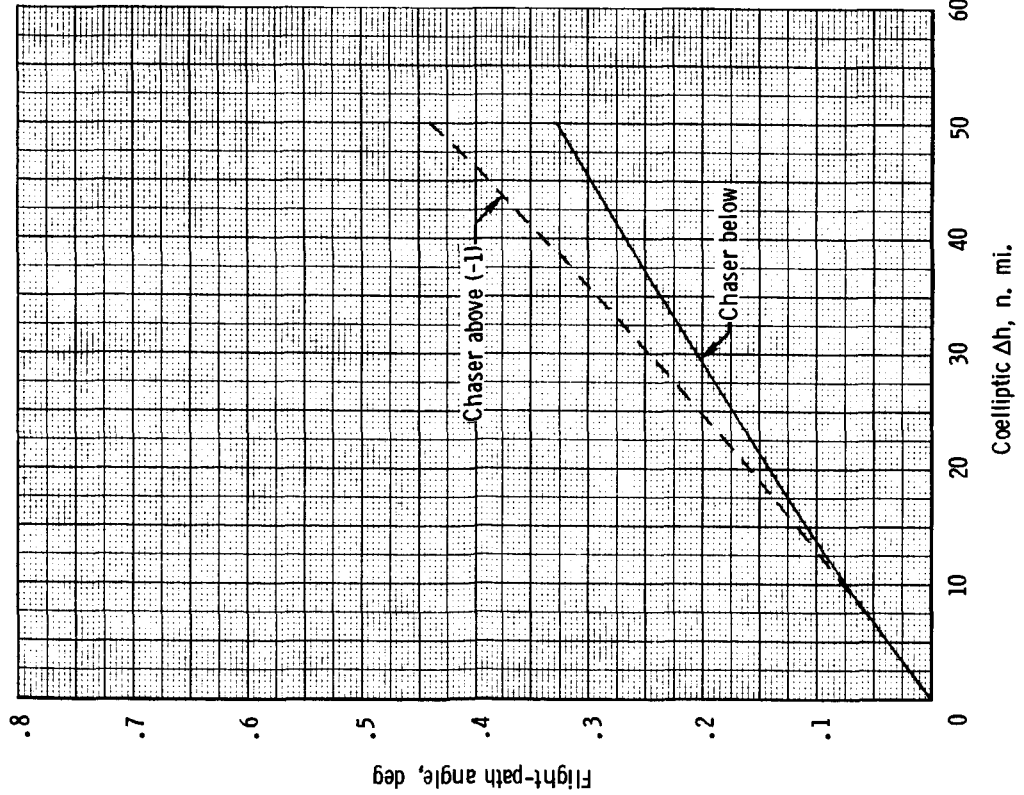
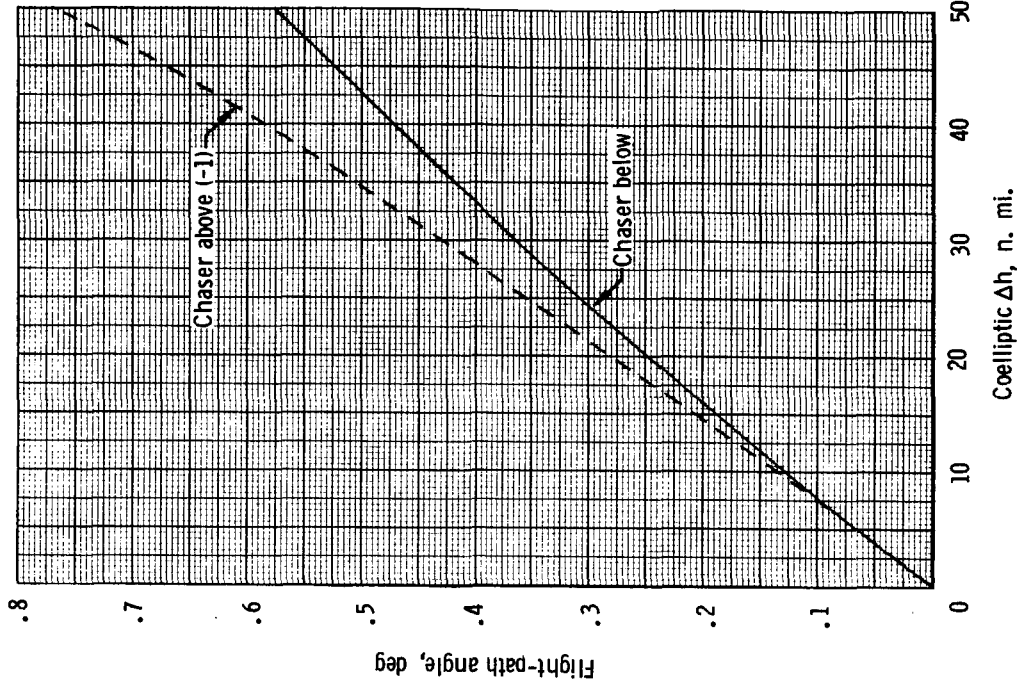


(a) Instantaneously after TPI.



(b) Instantaneously before TPI.

Figure 7. - Terminal phase true anomalies as a function of coelliptic Δh .



(a) Instantaneously after TPI.

(b) Instantaneously before TPF.

Figure 8. - Terminal phase flight-path angles as a function of coelliptic Δh .

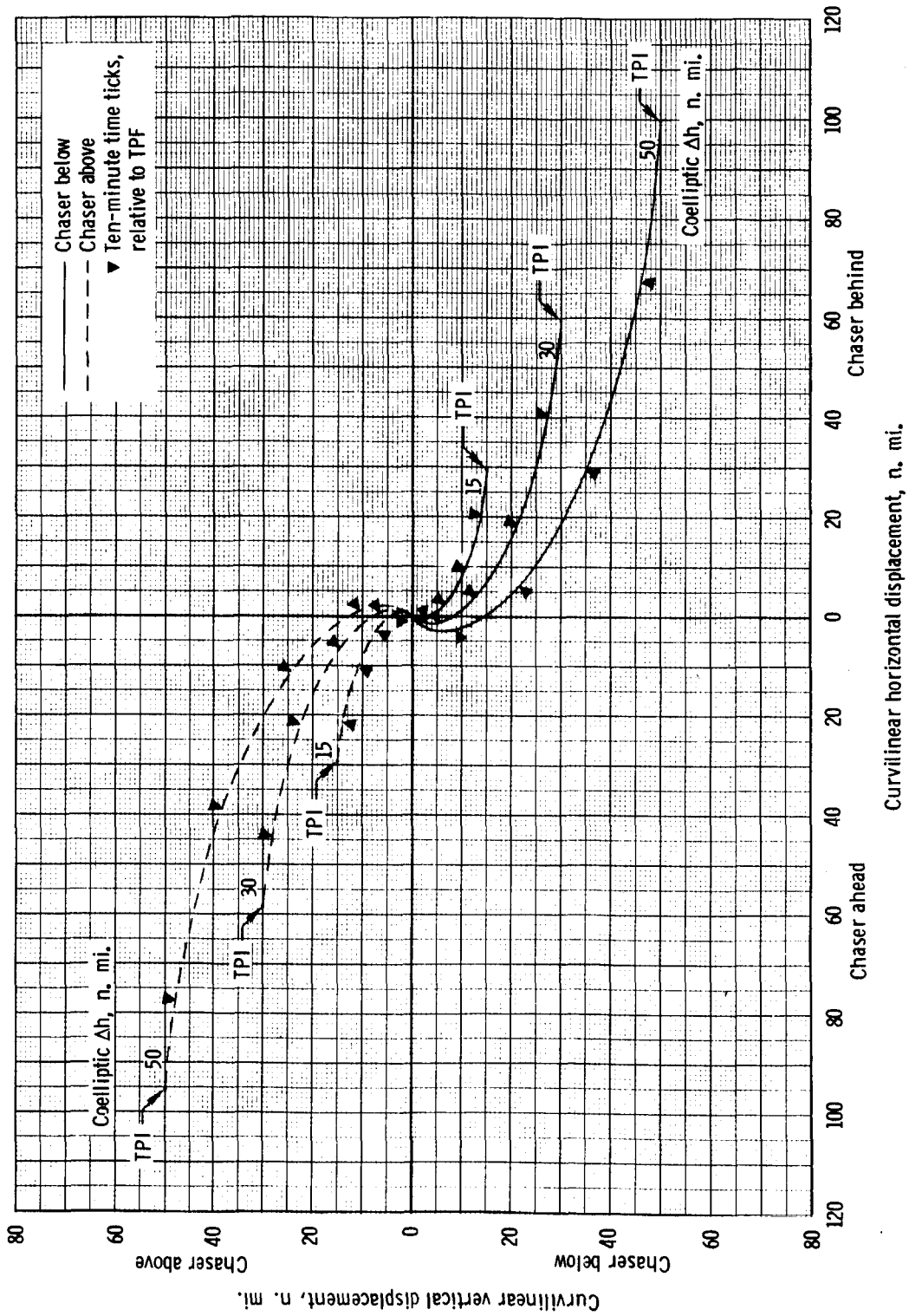
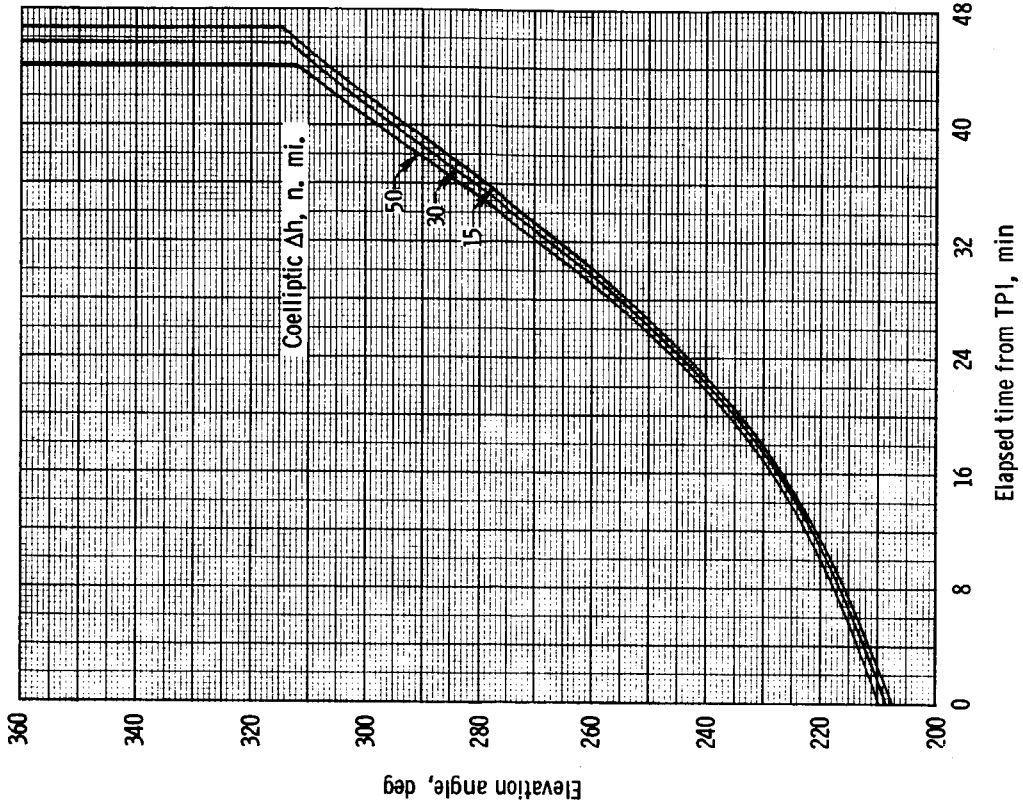
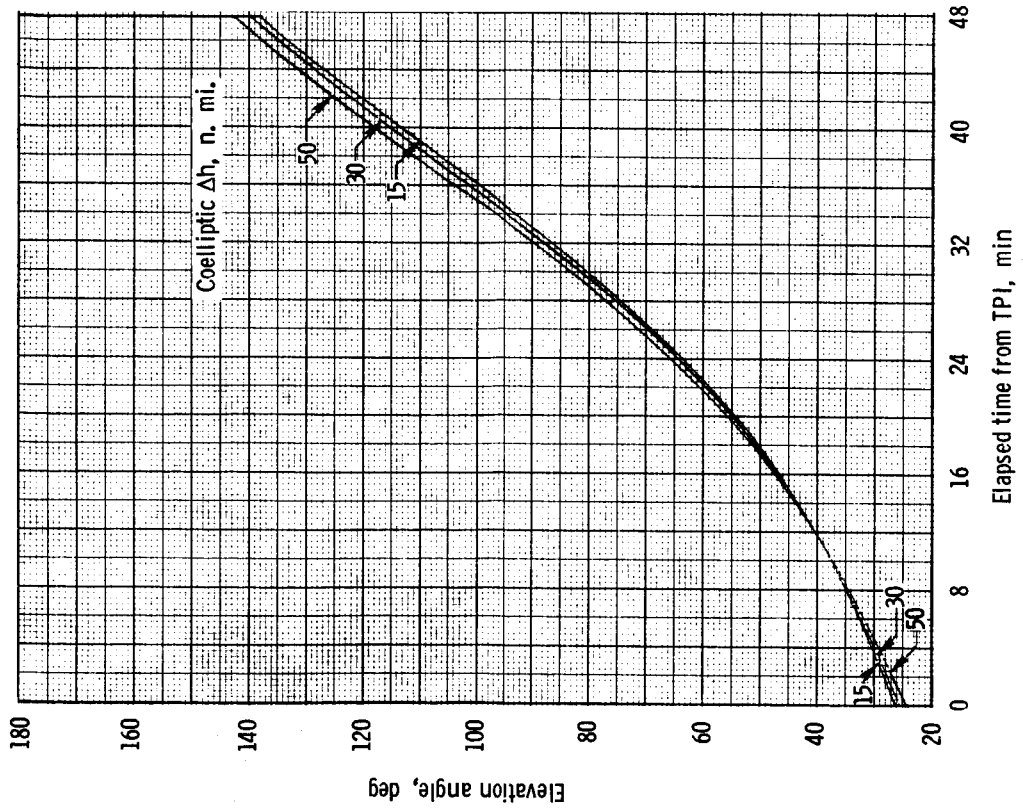


Figure 9. - Terminal phase relative motion curves (target-vehicle-centered curvilinear coordinate system).

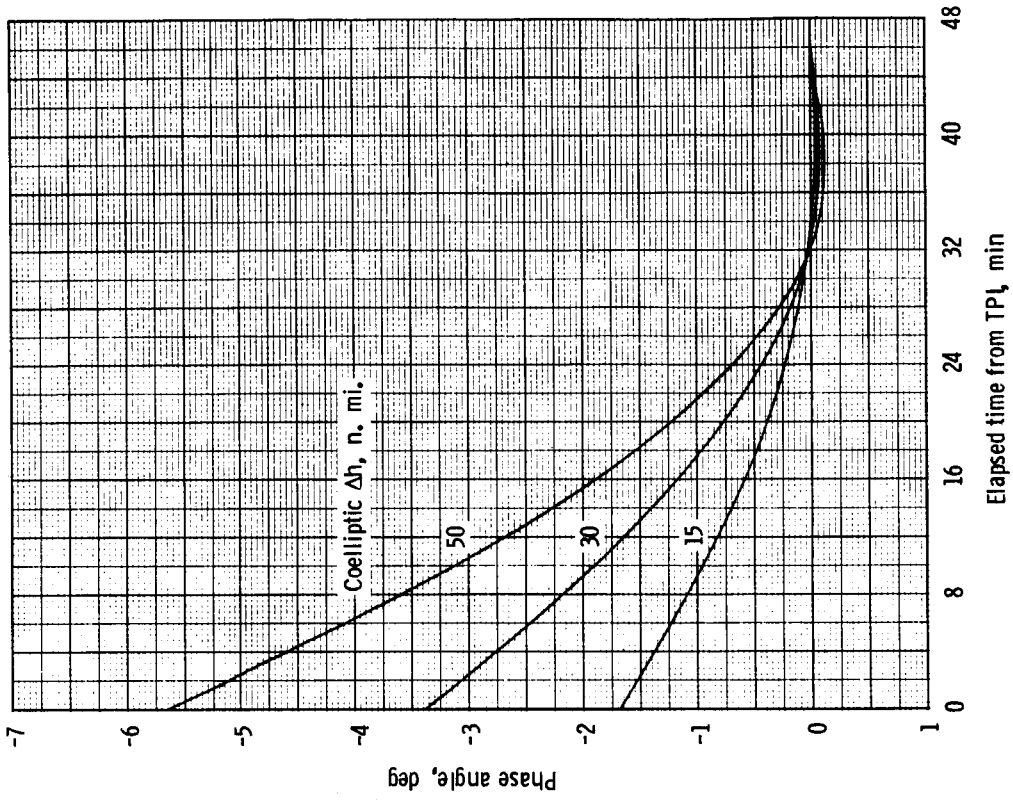


(a) Chaser below.

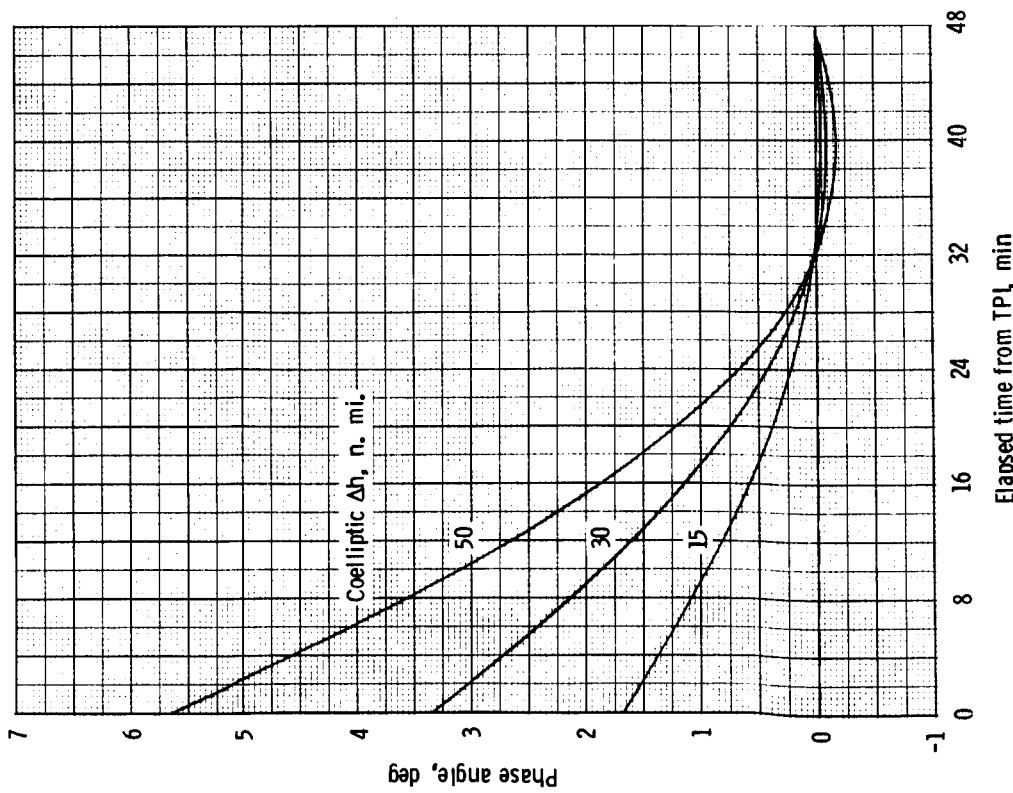


(b) Chaser above.

Figure 10. - Terminal phase time histories of elevation angle (chaser-to-target-vehicle).

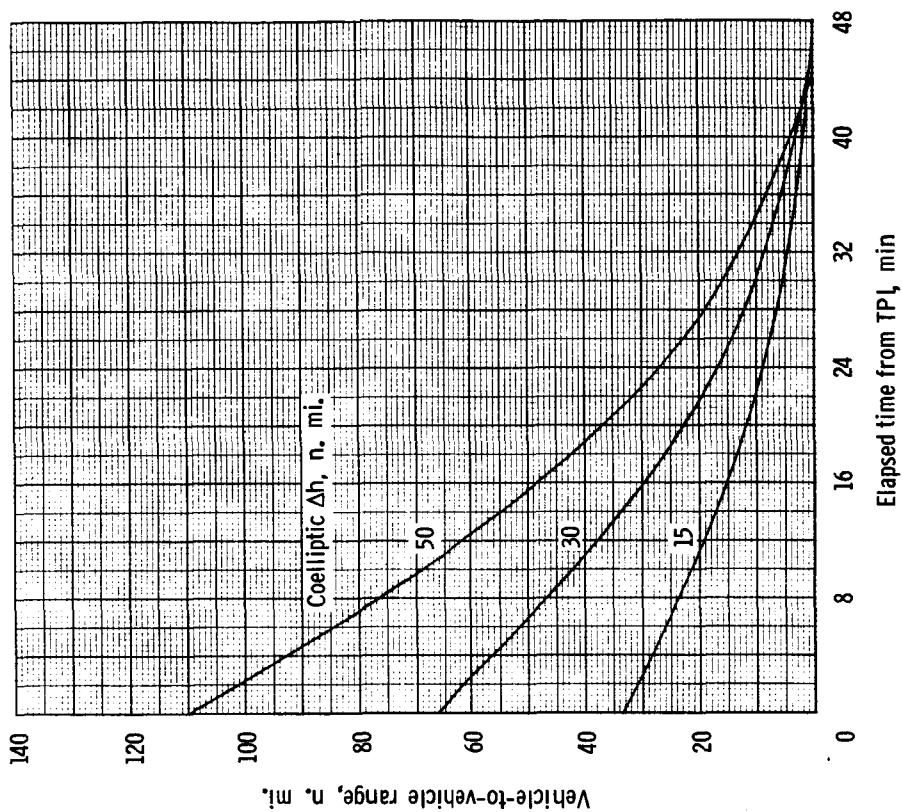


(a) Chaser below.

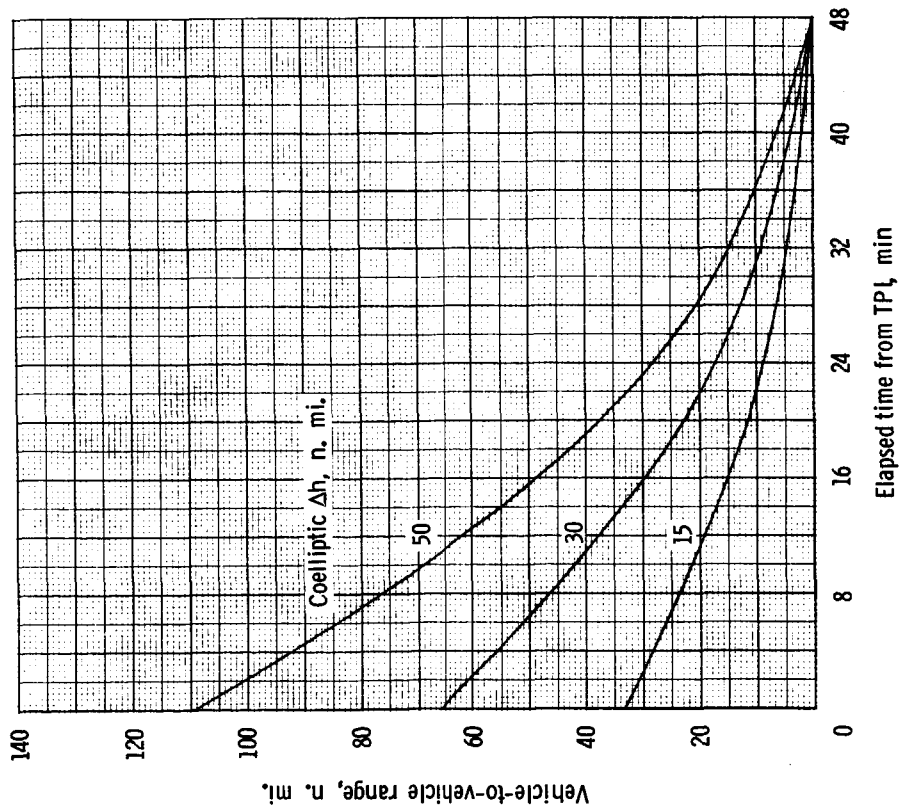


(b) Chaser above.

Figure 11.- Terminal phase time histories of phase angle (target-vehicle-ahead).



(a) Chaser below.



(b) Chaser above.

Figure 12. - Terminal phase time histories of vehicle-to-vehicle range.